Pramāṇa – J. Phys., Vol. 25, No. 4, October 1985, pp. 383–395. © Printed in India.

The neutron interferometer as a macroscopic quantum device

H RAUCH
Atominstitut der Österreichischen Universitäten Wien, Austria

Abstract. Neutron interferometry is a unique tool for investigations in the field of particle-wave dualism because massive elementary particles behave like waves within the interferometer. The invention of perfect crystal neutron interferometers providing widely separated coherent beams stimulated a great variety of experiments with matter waves in the field of basic quantum mechanics. The phase of the spatial and spinor wave function become a measurable quantity and can be influenced individually. High degrees of coherence and high order interferences have been observed by this technique. The 4π-symmetry of a spinor wave function and the mutual modulation of nuclear and magnetic phase shifts have been measured in the past. Recent experiments dealt with polarized neutron beams, which are handled to realize the spin-superposition of two oppositionally polarized subbeams resulting in a final polarization perpendicular to both initial beam polarizations. The different actions on the coherent beams of static (DC) and dynamic (HF) flippers have been visualized.

Keywords. Neutron interferometry; crystal optics; macroscopic quantum device; coherence measurement; spinor symmetry.

1. Introduction

The invention of perfect crystal neutron interferometry in 1974 (Rauch *et al* 1974; Bauspiess *et al* 1974) allowed the realization of experiments with matter waves having widely separated beam paths. Thermal neutrons turned out to be an ideal probe for crucial test experiments of quantum mechanics. These neutrons have a kinetic energy of about 0·025 eV, a velocity of about 2200 m/sec and according to the de Broglie relation (de Broglie 1923) an associated wavelength of about 1·8 Å.

A monolithic perfect silicon crystal with dimensions in the order of 10 cm serves as optical device for a coherent splitting, reflection and superposition of the neutron wave (figure 1). The theoretical framework for these processes is given by the dynamical diffraction theory first developed for x-ray diffraction (von Laue 1941; Zachariasen 1945). It can easily be extended to neutron waves by solving the Schrödinger equation for a strictly periodical potential which describes the perfect crystal (Rauch and Petrascheck 1978; Sears 1978).

The particle-wave dualism displays itself very directly because the neutron behaves inside the interferometer purely like a wave but its particle properties have to be transferred from the entrance to the exit, too. These particle properties are known to a high precision.

* Neutron mass (m = 1·674954320(61) g (Ramsey (1975) which becomes also visible by the action of gravity on its path (Koester 1976).
* Low energy neutron proton scattering is well described by classical collision laws.

The energy after collision depends on the scattering angle in laboratory frame like $E' = E_0 \cos^2\theta$.

* Magnetic moment ($\mu = -1{\cdot}91304211(88)\ \mu_K$ (Greene *et al* 1977, μ_K ... nuclear magneton) and the spin values ($\mathbf{s} = (1/2)\sigma h$, σ ... Pauli spin matrices).
* Charge and magnetic moment distribution indicate a mass radius of about 1 fm (Bilen'kaya and Kazarinov 1980).
* Neutron half life for β-decay ($T_{1/2} = 623{\cdot}6\ (6{\cdot}2)$ s, Wilkinson 1982).

The wave properties are described by the Schrödinger equation in time-dependent

$$H\psi = i\hbar \frac{\partial \psi}{\partial t}, \tag{1}$$

or time-independent form

$$H\psi = E\psi. \tag{2}$$

The plane wave solution $\psi = \exp[i(\mathbf{kr} - \omega t)]$ where $|\mathbf{k}| = 2\pi/\lambda$ does not define the particle in space and therefore a wave packet has to be constructed (Messiah 1965; Hittmair 1972)

$$\psi = \frac{1}{(2\pi)^{3/2}} \int A(\mathbf{k}') \exp[i(\mathbf{k}'\mathbf{r} - \omega t)]\, \mathrm{d}k'. \tag{3}$$

For a proper beam modelling $A(\mathbf{k}')$ can be assumed to have a Gaussian shape for all three diemensions centred around $\mathbf{k}_0$.

$$A(k') = \frac{1}{(2\pi\delta k^2)^{1/4}} \exp\left(-\frac{(k'-k_0)^2}{4\delta k^2}\right) \tag{4}$$

where δk is related to the full half width Δk (or $\Delta\lambda$) of the measurable momentum or wavelength distribution $W(k)$ as $\delta k = \Delta k/2\ (2\ln 2)^{1/2} = 0{\cdot}4246\,\Delta k$. Using the Heisenberg uncertainty relation one gets $\delta x(t)$ the spreading of the wave packet in space at time t after defining the packet at $t = 0$ with $\delta x(0)$

$$[\delta x(t)]^2 = [\delta x(0)]^2 + \left(\frac{\hbar t}{2m\delta x(0)}\right)^2 \tag{5}$$

It is worthwhile to note that for thermal neutron beams in most cases the second term dominates the spatial dimension of the packet. $A(\mathbf{k})$ is usually determined by the resolution function $W(\mathbf{k}) = |A(\mathbf{k})|^2$ of the experimental set-up. It is therefore defined for an ensemble of neutrons only. Nevertheless, it can be used to describe an individual neutron within a beam having this resolution function.

The wave and particle picture are linked together by the de Broglie (1923) relation

$$\lambda = 2\pi/k = h/mv, \tag{6}$$

where v is the group velocity.

2. Foundation of the coherent crystal optics

The solution of the stationary Schrödinger equation (equation (2)) for a strictly periodical potential which, in the neutron case, can be written in the form of a Fermi

pseudopotential

$$V(\mathbf{r}) = V(\mathbf{r}+\mathbf{R}_i) = \frac{2\pi\hbar^2}{m}\sum_i b_c\delta(\mathbf{r}-\mathbf{R}_i) \tag{7}$$

($\mathbf{R}_i$ is a lattice vector and b_c the coherent scattering length of crystal nuclei) gives near a Bragg position two strong internal wave fields. The two related waves have slightly different group velocity because one wave field has its nodes at the atomic position of the lattice while the second one has its nodes between the atomic positions. Applying the boundary conditions for a flat crystal slab in Laue position one obtains the wave functions in forward and Bragg direction (Rauch and Petrascheck 1978; Sears 1978)

$$\begin{aligned}\psi_0 &= v_0\psi_e = \left[\cos\left(A(1+y^2)^{1/2}\right] + \frac{y}{(1+y^2)^{1/2}}\right.\\ &\quad \left.\sin\left[A(1+y^2)^{1/2}\right]\right\}\exp(iPt)\psi_e,\\ \psi_H &= v_H\exp(2\pi iyt/\Delta_0)\psi_e = \left(-i\frac{\sin\left[A(1+y^2)^{1/2}\right.}{(1+y^2)^{1/2}}\right)\\ &\quad \exp\left[(it(P+2\pi iy/\Delta_0)\right]\psi_e.\end{aligned} \tag{8}$$

For an even (e.g. (220)) Si-reflection in symmetrical Laue position the parameters are given as

$$\begin{aligned}P &= -\frac{\pi y}{\Delta_0} - \frac{2\pi}{D_\lambda\cos\theta_B},\\ \Delta_0 &= \frac{\pi t}{A} = \frac{D_\lambda\cos\theta_B}{2} = \frac{k\cos\theta_B}{2b_cN},\\ y &= \frac{(\theta_B-\theta)k^2\sin 2\theta_B}{4\pi b_cN}.\end{aligned} \tag{9}$$

In this equation θ_B denotes the exact Bragg angle and N the particle density of the crystal. The small Debye-Waller correleation can be included to the coherent scattering length ($b_c \to b_c\exp(-w)$).

For the interferometer crystal (figure 1) relation (8) has to be used successively for the three crystal plates. The beams emerging behind the interferometer are composed of the two parts coming from beam paths I and II, respectively (Peterscheck 1976; Bauspiess *et al* 1976)

$$\begin{aligned}\psi_0 &= \psi_0^{\mathrm{I}} + \psi_0^{\mathrm{II}} = \left[v_0(y)v_H(y)v_{-H}(-y) + v_H(y)v_{-H}(-y)v_0(y)\right]\\ &\quad \times\exp\left[-2\pi iy(T+t)/\Delta_0\right].\psi_e\end{aligned} \tag{10}$$

and a similar relation holds for $\psi_H = \psi_H^{\mathrm{I}} + \psi_H^{\mathrm{II}}$. Combining (8) and (10) gives, for ideal geometry, the important relation

$$\psi_0^{\mathrm{I}} = \psi_0^{\mathrm{II}}, \tag{11}$$

and therefore

$$I_0 = |\psi_0^{\mathrm{I}} + \psi_0^{\mathrm{II}}|^2 = 4|\psi_0^{\mathrm{I}}|^2. \tag{12}$$

Particle conservation is guaranteed together with the beam in Bragg direction $I_H =$

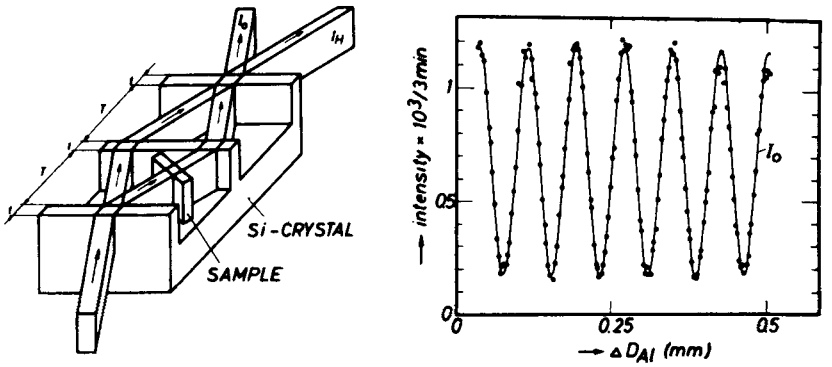

Figure 1. Sketch of a perfect crystal neutron interferometer (left) and a typical interference pattern (right).

$|\psi_H^I + \psi_H^{II}|^2$. The inclusion of wave packets or the spherical wave treatment do not change the relations substantially.

For a real system (11) becomes more complex due to various imperfections of the crystal, its dimensions, low frequency vibrations etc.

$$\psi_0^{II}/\psi_0^I = a \exp(i\phi) \tag{13}$$

and therefore

$$I_0 = |\psi_0^I + \psi_0^{II}| = (1 + a^2 + 2a\cos\phi)|\psi_0^I|^2. \tag{14}$$

Similar to optics a mutual coherence function can be defined

$$\gamma = \frac{2|\psi_0^I \psi_0^{II}|}{|\psi_0^I|^2 + |\psi_0^{II}|^2}. \tag{15}$$

3. Coherence measurements

For such measurements the phase relation between ψ_0^I and ψ_0^{II} has to be varied by the introduction of a sample having an index of refraction n and a thickness D. The index of refraction is given by the volume average of the interaction potential of (7) ($\overline{V} = 2\pi\hbar^2 b_c N/m$)

$$n = \frac{k}{k_0} = \left(1 - \frac{\overline{V}}{E}\right)^{1/2} \simeq 1 - \lambda^2 \frac{Nb_c}{2\pi}, \tag{16}$$

which is independent of the sample structure and is, for thermal neutrons, in the range of $n \sim 1 - 10^{-5}$. The phase difference is governed by the optical path length difference

$$\psi_0^{II'} = \psi_0^I \exp[-i(1-n)kD] = \psi_0^I \exp[-i\lambda b_c N D] = \psi_0^I \exp(i\chi), \tag{17}$$

and by varying D or N an intensity modulation occurs

$$\begin{aligned} I_0 &= |\psi_0^I + \psi_0^{II'}|^2 = 2|\psi_0^I|^2(1 + \cos Nb_c\lambda D) \\ &= 2|\psi_0^I|^2[1 + \cos(2\pi D/D_\lambda)]. \end{aligned} \tag{18}$$

If a sample is rotated in both coherent beams D denotes the difference of the sample thickness in both beams. The inclusion of the experimental imperfections (equation (13)) causes a reduction of the full beam modulation (equation (18)), but for a very well balanced neutron interferometer a performance rather close to the ideal one can be reached as shown in figure 1 (Rauch 1979).

The intensity modulation is about 90% and many characteristical interference experiments can be realized by varying the phase or putting absorbers into the beams (Rauch and Summhammer 1984).

The index of refraction (equation (16)) and the intensity modulation (equation (18)) depend on the neutron wavelength and therefore an average over the wavelength distribution has to be taken. For a Gaussian distribution function having a full half-width $\Delta\lambda$ the calculated intensity modulation now reads

$$\bar{I}_0 = \int I_0(\lambda) W(\lambda)\,\mathrm{d}\lambda = 2|\psi_0^{\mathrm{I}}|^2 \exp\left[-\left(1{\cdot}886\frac{D}{D_\lambda}\frac{\Delta\lambda}{\lambda}\right)^2\right]\cdot\left\{1+\cos\frac{2\pi D}{D_\lambda}\right\}. \tag{19}$$

It is seen that the beam resolution ($\Delta\lambda/\lambda$) reduces the modulation (coherence) mainly at high orders ($n = D/D_\lambda$) of the interferences. Additionally, it should be mentioned that the same result is obtained if wave packets (equation (3)) are used for ψ_0^{I} and ψ_0^{II} in (18) instead of $W(\lambda)$ in (19) because $W(\lambda) = |A(\lambda)^2|$.

The usual beam attenuation ($\sigma_r = \sigma_a + \sigma_{\mathrm{incoh}}$) due to absorption ($\sigma_a$) and incoherent scattering (σ_{incoh}) processes has also to be accounted for. It is described by a complex interaction potential and therefore by a complex index of refraction (18)

$$n \simeq 1 - \frac{\lambda^2 N}{2\pi}[b_c^2 - (\sigma_r/2\lambda)^2]^{1/2} + i\frac{\sigma_r N\lambda}{2\pi} \tag{20}$$

Using (16), (17) and (19) together yields (19)

$$\bar{I}_0 = 2|\psi_0^{\mathrm{I}}|^2 \exp[-\sigma_r ND/2]\exp\left[-\left(1{\cdot}886\frac{D}{D_\lambda}\frac{\Delta\lambda}{\lambda}\right)^2\right]$$
$$\{\cosh(\sigma_r ND/2) + \cos(2\pi D/D_\lambda)\}. \tag{21}$$

This gives a further limitation ($\sigma_r ND/2 \lesssim 1$) to the visibility of interference fringes. Related experiments have been performed using a highly monochromatic neutron beam ($\Delta\lambda/\lambda = 10^{-3}$) and thick samples (figure 2) (Rauch 1979; Rauch *et al* 1976). The theoretical values of (21) (full bars) agree rather well with the measured reduction of the intensity modulation. Interference fringes up to the 329th order have been observed from which an overall longitudinal coherence length of $500\lambda = 875$ Å can be extrapolated. This quantity is related to the monochromacy of the beam and the observable effects are equivalently describable by a distribution function or a wave packet representation of the wave function. The visibility of the interference pattern (equation (21)) depends on $\Delta\lambda$ (or Δk) and not on Δx and therefore the spatial spreading (equation (5)) does not influence this effect. Some further comments on this topic are given in the literature (Klein *et al* 1983; Hamilton *et al* 1983).

Uptil now we discussed the longitudinal coherence length. The transverse coherence length is determined by the multiple perfect crystal reflection at the interferometer plates. Due to the Pendellösung interference within the perfect crystal the reflectivity

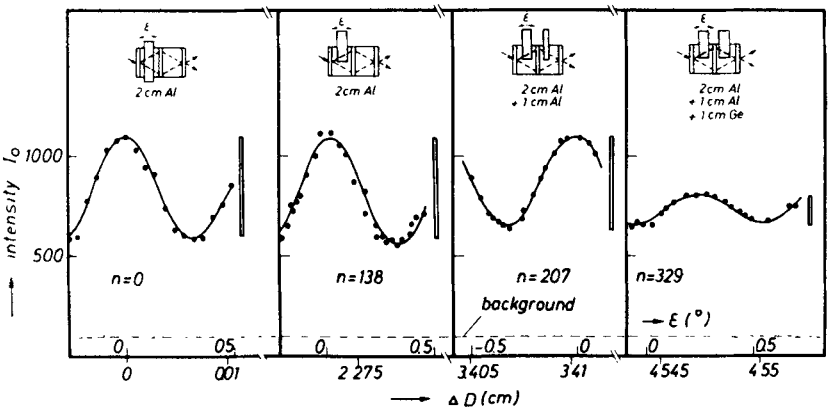

Figure 2. High order interferences and the reduction of the contract due to the wavelength spread of the beam (Rauch 1979).

curves show the typical Pendellösung pattern, which follows from (8) as

$$I_H \propto |\psi_H|^2 = \frac{\sin^2 A(1+y^2)^{1/2}}{1+y^2}. \tag{22}$$

The rocking curve of successive reflections is given by the convolution of such functions and shows a marked needle structure with a central peak having a width $\Delta\alpha \sim d_{hkl}/t$, which is in the range of 0·001 sec of arc (Bonse *et al* 1977, 1979; Petrascheck and Rauch 1984). These neutrons have a very well defined $\Delta k_T/k$-value ($\Delta k_T/k = 4{\cdot}3 \times 10^{-8}$) and show slit diffraction effects even at very wide slits ($a \gg \lambda$) whose diffraction pattern and broadening $\beta_{1/2}$ of the direct beam is given by the Frauenhofer formula (Shull 1969)

$$I(\beta) = I_0 \frac{\sin^2[\pi a \sin\beta/\lambda]}{(\pi a \sin\beta/\lambda)^2}, \tag{23}$$

$$\sin\beta_{1/2} = 0{\cdot}888\,\lambda/a.$$

To achieve the high angular resolution required to observe this narrow central peak a wedge-shaped sample is rotated around the beam axis between the plates of a monolithic designed triple reflection crystal. The angular deflection δ depends on the index of refraction, the apex angle (η) of the wedge and the rotation angle (ξ) around the beam axis (Bonse *et al* 1979)

$$\delta = \left[2(1-n)\,tg\frac{\eta}{2}\right]\sin\xi. \tag{24}$$

The experimental set-up and the results are shown in figure 3 (Rauch *et al* 1983). A beam broadening has been observed up to a slit width of 5 mm and a transversal coherence length of 6·5 mm can be deduced from these data. This value corresponds to $3{\cdot}7 \times 10^7$ times the neutron wavelength and is much larger than values reported before in the literature (Shull 1969; Scheckenhofer and Steyerl 1977). The coherence length in the vertical direction is usually quite small ($\sim$ 50 Å) because no real vertical collimation exists.

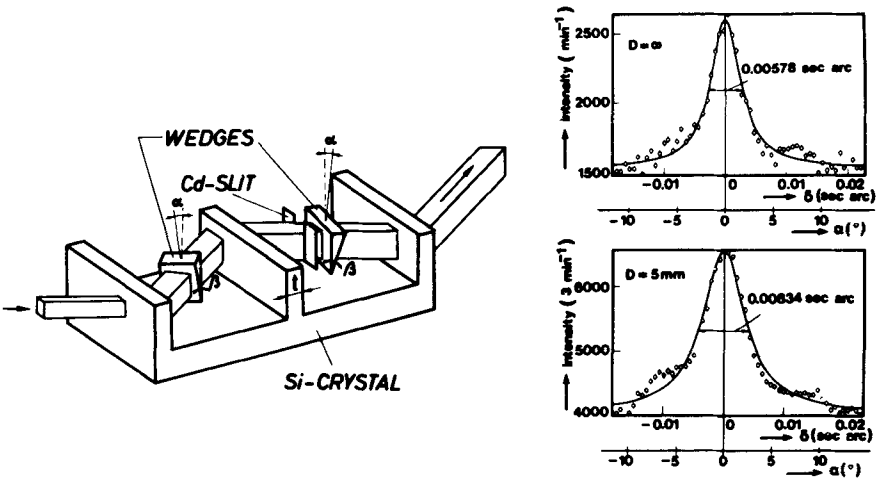

Figure 3. Experimental arrangement for the observation of the narrow central peak of multiple Laue rocking curves (left) and a typical slit diffraction pattern (Rauch *et al* 1983).

4. Spinor symmetry and spin superposition measurements

An important aim of neutron interferometry was the verification of the 4π-symmetry of a spinor wave function, which was treated as a kind of a "hidden" variable. The unitary rotation operator for a spinor wave function reads

$$\psi(\alpha) = \exp[-i\sigma\alpha/2]\psi(0), \tag{25}$$

where $\alpha = (\gamma/v)\int \mathbf{B}\,ds$ is the rotation angle around the magnetic field $\mathbf{B}$, γ is the gyromagnetic ratio, v is the velocity of the neutron. $\int ds$ is the path integral and σ are the Pauli spin matrices. Using this equation instead of equation (17) for the calculation of the intensity (equation (18)) one gets (Eder and Zeilinger 1976)

$$I_0 = 2|\psi_0^{\downarrow}|^2\left(1+\cos\frac{\alpha}{2}\right) \tag{26}$$

which shows the typical 4π periodicity. This result can also be obtained by an index of refraction formalism where the different interaction energies $\bar{V} = \pm\mu B$ of the two subbeams ($\pm$) constituting the beam are used to calculate the interference pattern from (16) and (18).

The 4π spinor symmetry effect appears for polarized and unpolarized beams as well, indicating the self-interference properties of the neutron within the interferometer. The first verification of the 4π-symmetry was achieved in 1975 using simple magnetic fields along one beam path (figure 4) (Rauch *et al* 1975; Werner *et al* 1975). More recently this experiment has been repeated by using well-defined magnetic fields within Mu-metal sheets (Rauch *et al* 1978). The periodicity factor extracted from these data using up-to-date values or the physical constants is (Rauch 1982)

$$\alpha_0 = 715{\cdot}87 \pm 3{\cdot}8 \text{ deg} \tag{27}$$

where the error bars indicate the simple σ-limits. In the meantime this 4π-symmetry has been verified by other techniques too (Klein and Opat 1976; Klempt 1976; Stoll *et al*

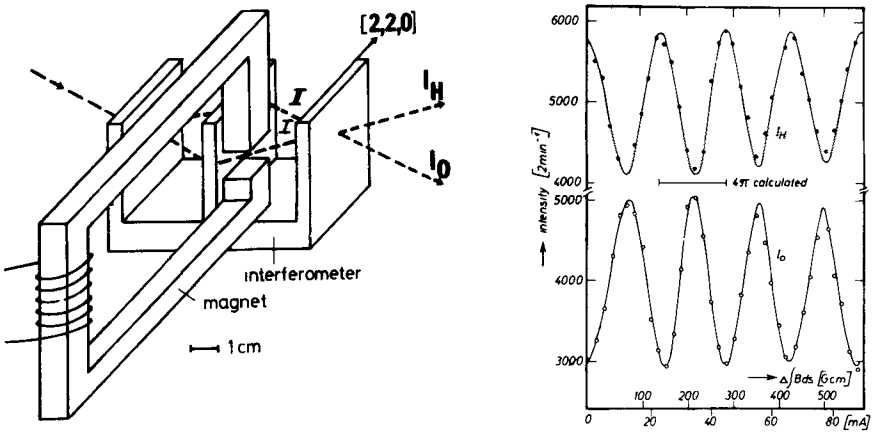

Figure 4. First observation of the 4π-symmetry of a spinor wave function (Rauch *et al* 1975).

1978). Small correction terms to (26) occur due to a slightly different transit time through the magnetic field of the two subbeams ($\pm$) (Bernstein 1979). If nuclear (equation (17)) and magnetic phase shifts occur simultaneously additional effects concerning intensity and polarization modulation were predicted (Eder and Zeilinger 1976; Zeilinger 1976) and have been verified experimentally (Badurek *et al* 1976).

Another important experiment dealt with the verification of the spin superposition law on a macroscopic scale. A polarized incident beam is split coherently and the polarization direction of one coherent beam is rotated by an angle π. Later it is superposed to the unchanged polarization state of the other beam. For this situation a polarization perpendicular to both initial polarization states is predicted (Wigner 1963; Zeilinger 1979; Eder and Zeilinger 1976). The unitary operator for nulcear and magnetic interaction (equations (17) and (25)) reduces in this case to

$$U = -i\sigma_x \exp(i\chi), \tag{28}$$

and the final polarization is calculated as

$$\mathbf{P} = \frac{\psi_0^{\mathrm{I}+}(1+U^+)\sigma(1+U)\psi_0^{\mathrm{I}}}{I_0} = \mathbf{e}_x \sin\chi - \mathbf{e}_y \cos\chi. \tag{29}$$

This effect has been verified recently (Summhammer *et al* 1982) and the characteristic results and experimental set-up are shown in figure 5. Polarized neutrons are first obtained from magnetic prism deflection (Badurek *et al* 1979) and then the polarization inversions within the interferometer and the three-dimensional polarization analysis behind the interferometer are achieved with static DC-flippers. The results show that the final polarization lies indeed with the (xy)-plane and the polarization vector can be rotated within this plane even by a scalar interaction χ only. Momentum conservation is preserved due to the beam polarization of the H-beam. This experiment shows that a pure state at the entrance is transformed to a pure state with another direction at the exit of the interferometer although the spin direction is affected in one coherent beam only. This allows the statement that each neutron has at the place of superposition information about the physical situation within both coherent and widely separated beams.

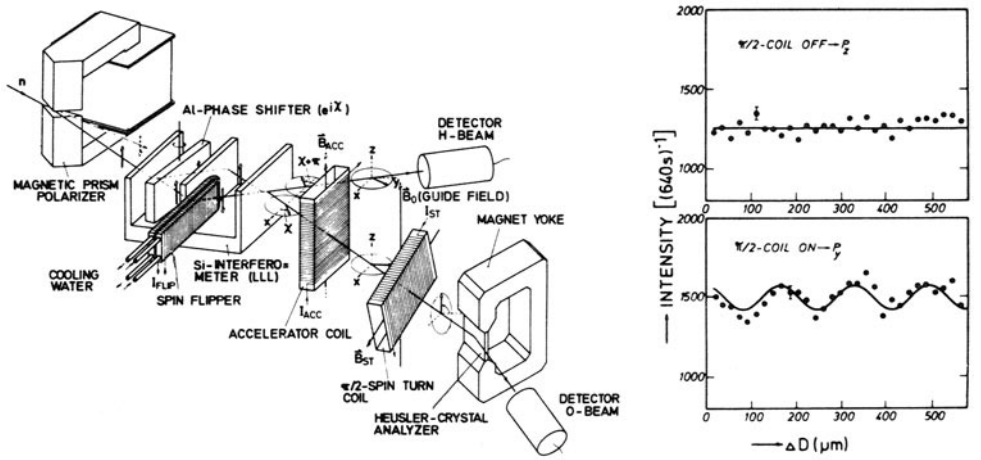

Figure 5. Experimental arrangement and results of the static spin superposition experiment (Summhammer *et al* 1982).

When a resonance spin flipper is used instead of the static flipper the physical situation changes drastically. Now a time-dependent interaction exists and therefore the time dependent Schrödinger equation has to be used to describe this phenomenon. In this case the spin reversal is accompanied with an exchange of a photon having an energy $\hbar\omega_{rf} = 2|\mu|B_0$ between the neutron and the resonance flipper (Drabkin and Zhitnikov 1960; Badurek *et al* 1980). This changes the total and potential energy but not the kinetic energy and therefore not the k-vector of the neutron. A change of the kinetic energy occurs at the entrance and at the exit due to the longitudinal Zeman splitting only. This behaviour has been verified experimentally by a separate experiment (figure 6) (Alefeld *et al* 1981).

The wave function behind the resonance flipper reads in the interferometer case as (Badurek *et al* 1983a, b)

$$\psi(\chi, \omega_{rf}) = \exp(i\mathbf{kr}) \exp(i\chi) \exp[-i(\omega - \omega_{rf})t] |\downarrow\rangle \tag{30}$$

and the superposition with the undisturbed wave function of beam I yields again a final polarization in the (xy)-plane which rotates in this plane in phase with the flipper field

$$\mathbf{P} = \begin{pmatrix} \cos(\chi - \omega_{rf} t) \\ \sin(\chi - \omega_{rf} t) \\ 0 \end{pmatrix} \tag{31}$$

This time-dependent rotation can be detected by a stroboscopic registration of the neutrons synchronized with the phase of the flipper field.

The parameters of the experiment (figure 7) were: guide field $B_0 = 190$ G, resonance frequency $\omega_{rf}/2\pi = 55{\cdot}4$ kHz, length of the flipper coil 1 cm, interval between registered time channels 9·03 msec, widths of time channels 4·51 msec, distance to the detector 25 cm which avoids frame overlap for a neutron beam having a mean wavelength $\lambda_0 = 1{\cdot}835$ Å and a spread of $\Delta\lambda/\lambda_0 = 0{\cdot}015$.

The experimental results also agree with the theoretical predictions and demonstrate that coherence can even be preserved when a real energy exchange occurs (Badurek *et al*

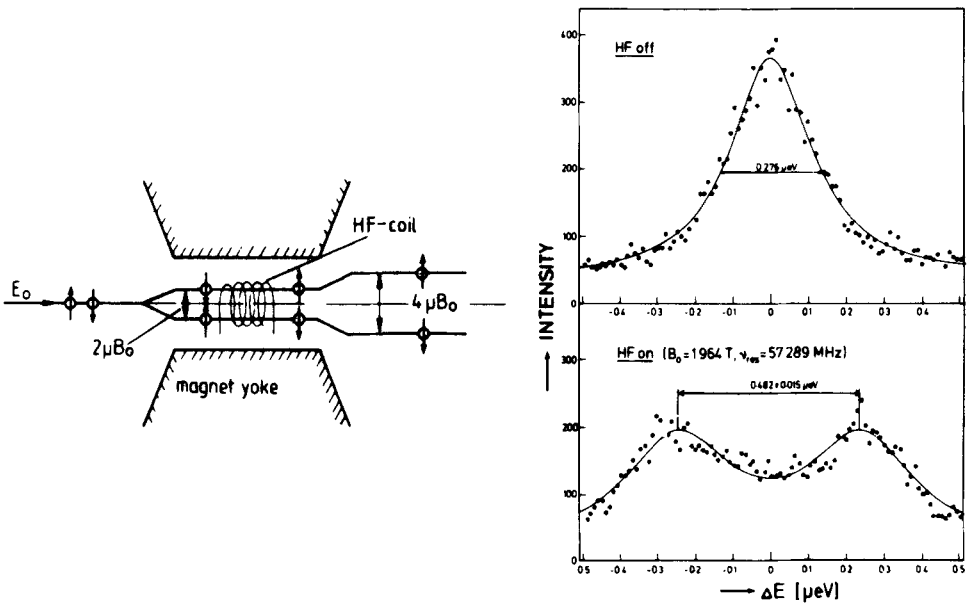

Figure 6. Verification of the coherent energy shift of a neutron magnetic resonance system (Alefeld *et al* 1981).

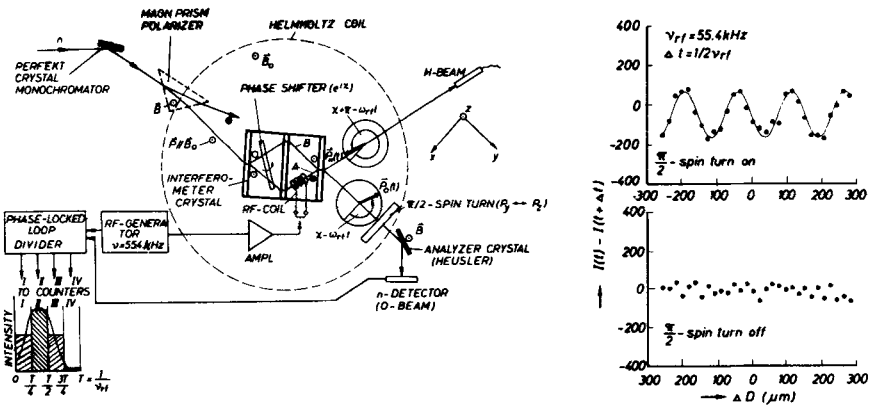

Figure 7. Experimental arrangement and result of the time dependent spin superposition experiment (Badurek *et al* 1983).

1983a). One might argue that besides the interference pattern the beam path can be detected by observing the added or missing photon of the resonance circuit or by measuring the change of the kinetic energy of the neutron behind the guide field where the different total energy is due to the longitudinal Stern-Gerlach effect transformed to a change of the kinetic energy of the neutrons (Alefeld *et al* 1981). But we note that the detection of a single photon transition simultaneously with the interference pattern is forbidden by the number phase uncertainty relation $\Delta N \Delta\phi \geqslant 1/2$, which is a most simple formulation of the more general number phase uncertainty relation (Jackiw 1968; Carruthers and Nieto 1968).

To observe the interference pattern the phase information must be at least half a

period and therefore a single missing or added photon cannot be detected and a simultaneous detection of the interference pattern and of the beam path becomes impossible. Several authors claim at this point that the limitations due to the Copenhagen interpretation can be overcome (Dewdney *et al* 1984), but that has to be shown in future.

One now might try to get the information about the path chosen by the neutron by measuring the change of the kinetic energy of these neutrons which passed through the resonance flipper. The related difference in the velocity of the neutrons is $\Delta v_{rf} = \mu B_0/mv$ (Badurek *et al* 1980a). It can be measured by a time-of-flight system placed at a distance Δl beyond the guide field region when the width of the incident beam is smaller than this quantity ($\Delta v < \Delta v_{rf}$). In order to accumulate the neutrons with the correct polarization phase in the correct time channels their widths have to fulfil the condition $\Delta t > \Delta l/\Delta v$, whereas these time channels have to be $\Delta t < 2\pi/\omega_{rf}$ to obtain the interference pattern. This runs into conflict with the momentum-position uncertainty relation $\Delta k \Delta l > 1/2$.

5. Summary and conclusions

Neutron interferometry permits the realization of many textbook experiments of quantum mechanics and therefore stimulates new discussions about the interpretation of quantum mechanics. Within the standard (Copenhagen) interpretation of quantum mechanics only probability amplitudes are relevant for the description of the coherent beams and no particle properties appear explicitly. Therefore the question how the non-separable neutron mass and the magnetic moment is transported through the interferometer is not answered. It is easily shown that only self-interference is important because even at a high flux reactor the mean time interval between the neutron counts is about 1·01 sec while the mean time-of-flight through the interferometer is in the order of 30 μsec. The wave packet describes a neutron but a neutron belonging to a certain ensemble and the parameters of the packet are determinable for the beam only. The introduction of the so-called "empty waves" (Selleri 1982) does not conflict with interpretation as long as no neutron is detected along the coherent beam path. In this case the wave field collapses and the interference pattern disappears. Many basic experiments of quantum mechanics which were Gedanken experiments so far could be realized by neutron interferometry but the questions concerning the particle-wave dualism and the Böhr-Einstein debate remain open for the future.

Acknowledgements

Most of the experimental results have been obtained at the neutron interferometer set up at the High Flux Reactor at Grenoble which is operated by a Dortmund-Grenoble-Wien interferometer team.

References

Alefeld B, Badurek G and Rauch H 1981 *Z. Phys.* **B41** 231
Badurek G, Rauch H and Summhammer J 1983a *Phys. Rev. Lett.* **51** 1015

Badurek G, Rauch H, Summhammer J, Kischko U and Zeilinger A 1983b *J. Phys.* **A16** 1133
Badurek G, Rauch H, Wilfing A, Bonse U and Graeff W 1979 *J. Appl. Crystallogr.* **12** 186
Badurek G, Rauch H and Zeilinger A 1980 *Z. Phys.* **B38** 303
Badurek G, Rauch H and Zeilinger A 1980 in *Neutron spin echo, Lect. Notes in Phys.* (ed.) F Mezei (Berlin: Springer Verlag) **128** 136
Badurek G, Rauch H, Zeilinger A, Bauspiess W and Bonse U 1976 *Phys. Rev.* **D14** 1177
Balcar E 1979 in *Neutron interferometry* (eds) U Bonse and H Rauch (Oxford: Clarendon Press) p. 252
Bauspiess W, Bonse U and Graeff W 1976 *J. Appl. Crystallogr.* **9** 68
Bauspiess W, Bonse U, Rauch H and Treimer W 1974 *Z. Phys.* **271** 177
Bernstein H J 1979 in *Neutron interferometry* (eds) U Bonse and H Rauch (Oxford: Clarendon Press) p. 231
Bernstein H J and Phillips A V 1981 *Sci. Am.* September
Bilen'kaya S I and Kazarinov Yu M 1980 *Sov. J. Nucl. Phys.* **32** 382
de Broglie L 1923 *Nature (London)* **112** 540
Bonse U, Graeff W, and Rauch H 1979 *Phys. Lett.* **A69** 420
Bonse U, Graeff W, Teworte R and Rauch H 1977 *Phys. Status Solidi.* **A43** 487
Carruthers P and Nieto M N 1968 *Rev. Mod. Phys.* **40** 411
Colella R and Overhauser A W 1980 *Am. Sci.* **68** 70
Dewdney C, Gueret P, Kyprianidis A and Vigier J P 1984 *Phys. Lett.* **A102** 291
Drabkin G M and Zhitnikov R A 1960 *Sov. Phys. JETP* **11** 729
Eder G and Zeilinger A 1976 *Nuovo Cimento* **B34** 76
Greenberger D E and Overhauser A W 1979 *Rev. Mod. Phys.* **51** 43
Greene G L, Ramsey N F, Mampe W, Pendlebury J M, Smith K and Perrin P 1977 *Phys. Lett.* **B71** 297
Halpern O 1952 *Phys. Rev.* **88** 1003
Hamilton W A, Klein A G and Opat G I 1983 *Phys. Rev.* **A28** 3149
Hanbury-Brown R and Twiss R Q 1957 *Proc. R. Soc. (London)* **A242** 300
Hanbury-Brown R and Twiss R Q 1957 *Proc. R. Soc. (London)* **A243** 291
Hittmair O 1972 *Lehrbuch der Quantenmechanik* (ed.) K Thiemig (München: Verlag)
Jackiw R 1968 *J. Math. Phys.* **9** 339
Klein A G and Opat G L 1976 *Phys. Rev. Lett.* **37** 238
Klein A G, Opat G L and Hamilton W A 1983 *Phys. Rev. Lett.* **50** 536
Klempt E 1976 *Phys. Rev.* **D13** 3125
Koester L 1976 *Phys. Rev.* **D14** 907
Krüger E 1980 *Nukleonika* **25** 889
von Laue M 1941 *Röntgenstrahlinterferenzen* (Leipzig: Akad. Verlagsges)
Marshall W and Lovesey S W 1971 *Theory of thermal neutron scattering* (Oxford: Clarendon Press)
Messiah A 1965 *Quantum mechanics* (Amsterdam: North Holland)
Nieden Th z and Weis O 1975 *Z. Phys.* **B21** 11
Petrascheck D 1976 *Acta Phys. Austr.* **45** 217
Petrascheck D and Rauch H 1976 Theorie des interferometers, AIAU-Report 76401, Atominstitut Wien
Petrascheck D and Rauch H 1984 *Acta Crystallogr.* **A40** 445
Ramsey N F 1975 in *Fundamental physics with reactor neutrons and neutrinos* (ed.) T von Egidy (Bristol and London: Institute of Physics) p. 61
Rauch H 1979 in *Neutron interferometry* (eds) U Bonse and H Rauch (Oxford: Clarendon Press) p. 161
Rauch H 1982 *Hadronic J.* **5** 729
Rauch H, Badurek G, Bauspiess W, Bonse U and Zeilinger A 1976 *Proc. Int. Conf. Interaction Neutrons with Nuclei* Lowell/MA, Vol. 2, p. 1027
Rauch H, Kischko U, Petrascheck D and Bonse U 1983 *Z. Phys.* **B51** 11
Rauch H and Petrascheck D 1978 in *Neutron diffraction Top. Curr. Phys.* (ed.) H Dachs (Berlin: Springer Verlag) **6** 303
Rauch H and Summhammer J 1984 *Phys. Lett.* **104** 44
Rauch H, Treimer W and Bonse U 1974 *Phys. Lett.* **A47** 369
Rauch H, Wilfing A, Bauspiess W and Bonse U 1978 *Z. Phys.* **B29** 281
Rauch H, Zeilinger A, Badurek G, Wilfing A, Bauspiess W and Bonse U 1975 *Phys. Lutt.* **A54** 425
Scheckenhofer H and Steyerl A 1977 *Phys. Rev. Lett.* **39** 1310
Sears V F 1978 *Can. J. Phys.* **56** 1261
Selleri F 1982 *Ann. Foundation L. de Broglie* **7** 45
Shull C G 1969 *Phys. Rev.* **179** 752

Silverman M P 1980 *Eur. J. Phys.* **1** 116
Stoll M E, Wolff E K and Mehring M 1978 *Phys. Rev.* **A17** 1561
Summhammer J, Badurek G, Rauch H and Kischko U 1982 *Phys. Lett.* **A90** 110
Werner S A 1980 *Physics Today* December
Werner S A, Colella R, Overhauser A W and Eagen C F 1975 *Phys. Rev. Lett.* **35** 1035
Wigner E P 1963 *Am. J. Phys.* **31** 6
Wilkinson D H 1982 *Nucl. Phys.* **A377** 474
Zachariasen W H 1945 *Theory of x-ray diffraction in crystals* (London: John Wiley)
Zeilinger A 1976 *Z. Phys.* **B25** 97
Zeilinger A 1979 in *Neutron interferometry* (eds) U Bonse and H Rauch (Oxford: Clarendon Press) p. 241